Broad and Intense Radiation Accompanying Multiple Volume Reflection of Ultrarelativistic Electrons in a Bent Crystal

L. Bandiera, E. Bagli, V. Guidi, and A. Mazzolari
INFN Sezione di Ferrara, Dipartimento di Fisica, Università di Ferrara, Via Saragat 1, 44122 Ferrara, Italy

A. Berra, D. Lietti, and M. Prest
Università dell'Insubria, Via Valleggio 11, 22100 Como, Italy, and INFN Sezione di Milano Bicocca, Piazza della Scienza 3, 20126 Milano, Italy

E. Vallazza
INFN Sezione di Trieste, Via Valerio 2, 34127 Trieste, Italy

D. De Salvador
INFN Laboratori Nazionali di Legnaro, Viale dell'Università 2, 35020 Legnaro, Italy, and Dipartimento di Fisica, Università Di Padova, Via Marzolo 8, 35131 Padova, Italy

V. Tikhomirov
Research Institute for Nuclear Problems, Belarusian State University, Minsk, Belarus
(Received 28 June 2013; published 18 December 2013)

The radiation emitted by 120 GeV/c electrons traversing a single bent crystal under multiple volume reflection orientation is investigated. Multiple volume reflection in one crystal occurs as a charged particle impacts on a bent crystal at several axial channeling angles with respect to a crystal axis. The resulting energy-loss spectrum of electrons was very intense over the full energy range up to the nominal energy of the beam. As compared to the radiation emission by an individual volume reflection, the energy-loss spectrum is more intense and peaks at an energy 3 times greater. Experimental results are compared to a theoretical approach based on the direct integration of the quasiclassical Baier and Katkov formula. In this way, it is possible to determine the mean number of photons emitted by each electron and, thus, to extract the single-photon spectrum, which is broad and intense. The soft part of the radiation spectrum is due to the contribution of coherent interaction between electrons and several reflecting planes intersecting the same crystal axis, whereas the hard part is mainly connected to coherent bremsstrahlung induced by correlated scattering of electrons by atomic strings (string of strings scattering and radiation). The radiation generation by multiple volume reflection takes place over a broad angular range of the incident beam with respect to coherent bremsstrahlung and channeling radiation in straight crystals. Therefore, this type of radiation can be exploited for applications, such as beam dump and collimation devices for future linear colliders.

DOI: 10.1103/PhysRevLett.111.255502 PACS numbers: 61.85.+p, 29.27.−a

Hard x and γ radiations are usually generated by ultrarelativistic electrons passing through strong magnetic fields of undulators and wigglers, which allows the reaching of photon energies of hundreds keV at modern synchrotrons [1] and will allow tens MeV in the polarized γ-ray sources for positron production in future linear colliders [2]. Harder gamma quanta are typically produced through electron bremsstrahlung in matter, though mostly soft photons are emitted via bremsstrahlung in an amorphous material.

With the aim of increasing the intensity of hard photoproduction, coherent effects in crystals, e.g., coherent bremsstrahlung (CB) and channeling radiation (CR), can be utilized. Such possibilities can be exploited for applications such as a positron source or as an innovative scheme for crystal-assisted collimation in future electron-positron linear colliders. Moreover, coherent effects in radiation and pair production could increase the rate of electromagnetic (e.m.) showers by many times as compared to the same process in amorphous targets [3–5], leading to the possibility of exploitation of coherent effects in crystal-based electromagnetic calorimeters. However, all coherent radiation effects in straight crystals manifest themselves within a narrow angular region, which becomes still narrower as the beam energy increases [6], thus constraining the exploitation of such phenomena for applications.

A possibility to overcome such limitations is offered by the usage of a coherent effect that is an exclusive feature of curved crystals, i.e., volume reflection (VR). Coherent effects in bent crystals have been known since 1976, when the possibility to steer channeled particles in bent crystals was proposed [7]. VR was predicted through

simulations in 1987 [8] and consists in the reversal of the transverse momentum of over-barrier particles via interaction with the planar potential barrier at the tangency point of the trajectory with curved planes. As a result, VR particles are deflected by an angle of the order of the Lindhard angle [9] to a direction opposite that of crystal bending. VR is characterized by a wider angular acceptance than that for channeling, being equal to the bending angle of the crystal. The radiation accompanying VR has been investigated [10–12], and it turned out that its angular acceptance considerably exceeds those for CB and CR in a straight crystal [10,13,14]. Another advantage of radiation in VR geometry is its weak dependence on a particle's trajectory and charge.

Despite many advantages, VR radiation is limited by the relatively weak strength of the field of crystal planes, which may limit the possibility of high-intensity γ production through VR. In order to increase the intensity of radiation in bent crystals, one can take advantage of the recently observed effect of multiple volume reflection in one crystal (MVROC) [15]. MVROC has already been studied at CERN with the purpose of increasing the deflection angle of VR, for either positive [16] or negative particles [17,18]. MVROC occurs in a bent crystal when the particles move at few channeling angles with respect to a crystal axis, when correlated scattering of particles by neighboring atomic strings [the so-called "string of strings" (SOS) scattering [9]] assures the possibility of repeated VR from the planes sharing the same axis, leading to a multireflection process [15]. By a combination of the wealth of planar reflections occurring for MVROC with the contribution of atomic strings, the expected spectral intensity should be very strong as compared to that of an individual VR. Furthermore, since the axial electric field is 6 times stronger than that for the planes, the SOS contribution should considerably increase the probability of hard-photon emission [19]. Moreover, the radiation emission accompanying MVROC preserves the advantages of VR, i.e., a wide angular acceptance and weak dependence on particle's motion and charge. In this Letter, we present an investigation on the radiation spectrum obtained through the interaction of 120 GeV/c electrons with a bent Si crystal under MVROC condition.

Figure 1(a) displays the [111] axis in Si and the incidence angles Θ_{X0}, Θ_{Y0}, of a particle trajectory at the entry face of a crystal. Figure 1(b) illustrates the working principle of MVROC, studied in terms of the vertical ψ_Y and horizontal ψ_r particle deviation angles from the initial direction, as measured in the reference system rYz comoving with a particle shifting along the bent [111] crystal axis. The initial values of the ψ_r and ψ_Y angles are equal to those of particle incidence (Θ_{X0}, Θ_{Y0}). Since the angle $\psi_r \simeq \Theta_{x0} - z/R$ decreases with z, the particle trajectory becomes sequentially parallel to several sets of planes. In this space, any VR results in a shift orthogonal to the plane of reflection. In order to maximize the horizontal and simultaneously minimize the vertical deflection angle, Θ_{X0} and Θ_{Y0} must satisfy the following conditions [15,20]:

$$\Theta_{X0} = \varphi/2, \qquad 3\theta_{c,a} \leq \Theta_{Y0} < \varphi \tan\alpha_{\rm pl}/2, \qquad (1)$$

with $\varphi = l/R$ being the bending angle of the crystal with thickness l, $\theta_{c,a}$ the axial channeling angle, and $\alpha_{\rm pl}$ the inclination angle of the strongest skew planes, such as the $(10\bar{1})$ and $(01\bar{1})$ the electron planes in Fig. 1(b). The equality in Eq. (1) assures symmetric deflection in the plane of bending, whereas the inequalities provide nearly planar motion in the field of atomic strings under SOS orientation (left) and the involvement of the strongest crystal planes into the reflection process (right). Below, we provide some considerations about the expected radiation emitted by 120 GeV/c electrons under MVROC conditions. More details can be found in Ref. [21].

The generation of radiation at ultrahigh energies under MVROC conditions encompasses different types of

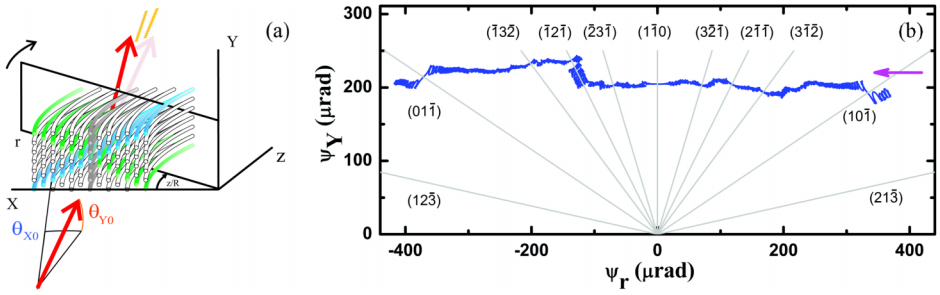

FIG. 1 (color online). An electron hits the crystal at a small angle with respect to the [111] axis and experiences VR from both the *vertical* $(1\bar{1}0)$ and numerous skew planes. (a) The comoving reference system rYz rotates with the bent axis direction z as the electron is moving through the crystal. (b) Evolution of particle transverse velocity in the rY plane, simulated in the averaged axial potential, taking into account the contribution of incoherent scattering. The arrow indicates the e^- transverse direction during the motion. The vertical projections of the angles of reflection from symmetric skew planes nearly compensate each other whereas the horizontal ones sum up leading to the MVROC effect. It also illustrates an example of the volume capture of electrons into a channeling regime by the $(\bar{1}2\bar{1})$ plane caused by a drop of the electron's transverse energy due to incoherent scattering by nuclei or radiative cooling [37]. However, volume capture occurs with low probability at 100 GeV, and therefore, it does not significantly affect the radiation emission.

emission mechanisms, sequentially occurring along the motion such as in the case of VR [13]. For VR, far from the reflection point, the angle between bent planes and particle motion ψ is greater than $V_{0,p}/m$, $V_{0,p}$ being the (110) planar potential well depth and m the electron mass, ensuring the dipole approximation to be valid so that CB theory holds [3–5]. While approaching the reflection point, the amplitude of the quasioscillatory motion of particles crossing the planes increases, leading to a deflection angle $\Delta\theta > 1/\gamma_{\text{Lorentz}}$. Therefore, more harmonics can be emitted, and the radiation process turns to a synchrotronlike process. As a result of multiple reflections, the role of synchrotronlike radiation increases under MVROC conditions.

Since MVROC occurs at relatively small angles of the particle trajectory with respect to a crystal axis, electrons experience the so-called scattering by SOS [9], rather than scattering by the smooth crystal planes. At very high energies, SOS radiation under MVROC conditions can be characterized by either an intermediate regime ($\psi \sim V_{0,a}/m$) between dipole and synchrotronlike or a quasidipole regime ($\psi > V_{0,a}/m$) for which the *modified* CB theory is applicable [5,19]. The only way to quantitatively account for all regimes is to use the quasiclassical operator method introduced by Baier and Katkov (BK) [5].

An experiment to investigate the e.m. radiation generated by 120 GeV/c electrons under MVROC has been built up at beam line H4 at CERN-SPS. The experimental setup of Ref. [14] was upgraded with a new trigger system, and a new electromagnetic calorimeter [22–24], which enabled us to record the full energy-loss spectrum up to the nominal energy of the beam by measuring the sum of the energies of all photons emitted by each electron.

Deflection was measured by a Si-based telescope system [25] with an angular resolution of 5 μrad, limited by multiple scattering of particles in the detectors and in the air. Beam divergence was 50 and 65 μrad in the horizontal and vertical directions, respectively. A $70 \times 2 \times 0.3$ mm^3 striplike Si crystal with the largest faces oriented parallel to the (110) planes was used. The crystal was fabricated according to the procedure described in Refs. [26,27] and bent through anticlastic deformation [28] to a curvature radius $R = (2.71 \pm 0.07)$ m.

Before the measuring of the radiation spectra, the particle dynamics was studied in order to ensure the proper experimental conditions for MVROC. The crystal was first tested vs VR onto the $(1\bar{1}0)$ vertical planes. A Gaussian fit to the reflected beam distribution yielded a mean deflection angle $\Theta_{\text{VR}} = (-11.4 \pm 0.7)$ μrad (see Fig. 2 dash-dotted line), consistent with the results of Ref. [29].

Then, the crystal was aligned with the beam to fulfill Eq. (1) for optimal MVROC, i.e., for horizontal and vertical incidence angles of $\Theta_{X0} = (365 \pm 5)$ μrad and $\Theta_{Y0} = (205 \pm 10)$ μrad, respectively. The mean deflection angle in the horizontal direction was

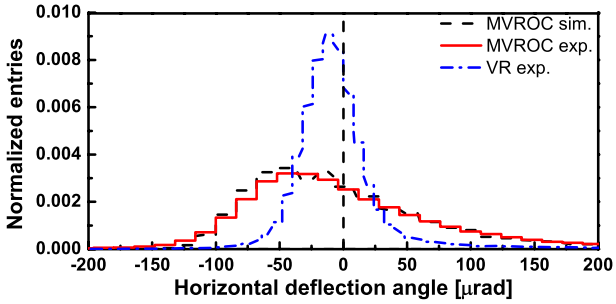

FIG. 2 (color online). Distribution of the horizontal deflection angle of particles interacting with the crystal aligned on VR (dot-dashed line) and MVROC (experimental and simulated results; solid and dashed lines, respectively).

$\Theta_{\text{MVROC}} = (-43.1 \pm 2.2)$ μrad (see Fig. 2 solid line), corresponding to $3.8\Theta_{\text{VR}}$. Deflection efficiency, as computed in Ref. [29], was $\varepsilon_{\text{vr}} = (85 \pm 2)\%$. The comparison between experimental results and the value calculated through the Monte Carlo method of Ref. [20] (dashed line of Fig. 2) shows a good agreement.

Figure 3 displays the experimentally recorded energy-loss distributions under VR (circles with bars) and MVROC conditions (squares with bars). The details about the procedure carried out to determine the distribution $(dn/dE)E$ vs the energy lost by electrons E are in Ref. [14]. A background contribution produced by the material (detectors, etc.) placed before the bending magnet is included in the experimental data and, thus, will be taken into account in the theoretical calculations [21]. As expected, measured spectral intensities were much more higher than the Bethe-Heitler (BH) value (see Fig. 3 solid line), typical for bremsstrahlung in amorphous materials. As the energy loss exceeded 105 GeV, experimental spectra vanished instead to attain the BH value. This feature is explained by the lack of data in the region of high-energy loss due to the saturation of the calorimeter, which reduced the spectral intensity at such energies [22]. The energy-loss spectrum under MVROC conditions exceeds that for VR beyond 10 GeV, being 3 or 4 times stronger within 60 GeV $\leq E \leq$ 80 GeV, and peaks at an energy 3 times greater.

Figure 3 also shows the energy-loss distribution simulated for MVROC condition (circles), performed through the method of direct integration of BK formula (DIBK) of Ref. [21]. In order to take into consideration multiple photon emission, the particle trajectories were divided into a few tens of intermediate-length parts, each of which was much longer than the radiation formation length and much shorter than the typical distance between two sequential photon emissions. Direct comparison of the outcomes by the DIBK method and the experimental results highlights a good agreement.

The single-photon spectrum (see Fig. 4 solid line) is more useful than energy-loss distribution to study the relative contributions of axial and planar fields to the radiation spectrum. According to the previous simulations

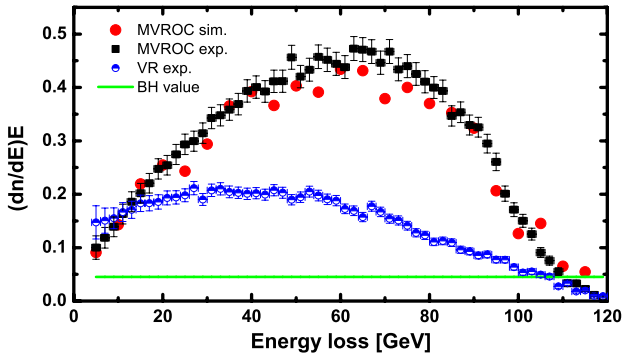

FIG. 3 (color online). Energy-loss spectra for 120 GeV/c electrons in the bent crystal; VR experimental results (circles with bars); amorphous estimation (solid line); MVROC experimental results (squares with bars) and DIBK (circles) simulations, carried out for 10^4 electron trajectories.

(see Fig. 4 in Ref. [30]), the greater intensity for MVROC than for VR in the soft-medium region of the spectra (<30 GeV) naturally arises from the contribution of several reflecting planes. In more detail, the greater intensity in the soft region (<20 GeV) is due to synchrotronlike photons, formed in the field of one plane in the region of reflection. Far from the latter, CB-like and, thus, harder photons (20 GeV $\leq \omega \leq$ 30 GeV) are emitted in the field of several neighboring atomic planes. In fact, the formation of photons in this medium-energy range is simultaneously determined by both SOS scattering and planar field contribution. Finally, harder photons ($\omega \geq$ 30 GeV) are emitted due to the SOS CB-like process in the field of axis [19], explaining the much stronger intensity of radiation accompanying MVROC in the hard region of the spectrum. One of the consequences of the multiple reflections is the greater number of soft photons than that for a single VR, leading to a mean number of photons emitted by each

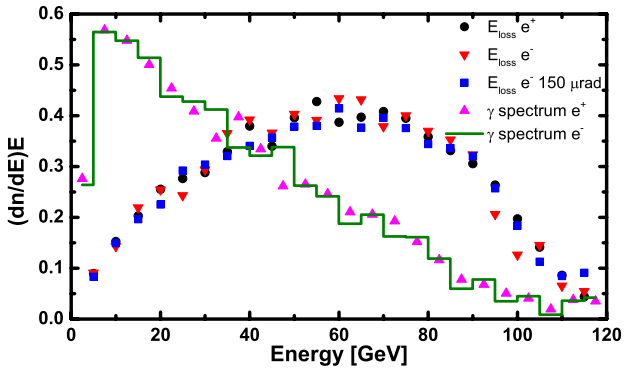

FIG. 4 (color online). Energy-loss distribution and single-photon spectrum for 120 GeV/c electrons (reverse triangles and solid line) and positrons (circles and triangles) simulated at the same experimental conditions of the MVROC plot (circles) in Fig. 3. Simulated energy-loss distribution for an electron beam with a divergence of 150 μrad (squares). Simulations were carried out for 10^4 particle trajectories.

particles (multiplicity factor) equal to 2.2/e^- for $\omega >$ 1 GeV, which is greater than the value for a single VR (see Ref. [21]). This circumstance explains the difference between the single-photon and energy-loss spectra.

The most important advantage of MVROC consists of a wide angular acceptance; i.e., the particles impinging on the crystal far from planes sharing the same axis can be multireflected during their motion due to the crystal bending. As described above, the radiation mechanisms change during the particle motion, depending on the direction of the particle's trajectory with respect to crystal planes and axis. The main point is that the dynamics of particles under MVROC conditions is similar for different incidence angles within the total angular acceptance. Similar particle's dynamics means similar radiation generation. Owing to the good agreement between experimental results and simulations, we investigated through simulations the robustness of radiation generated in MVROC orientation vs beam charge and divergence. Figure 4 displays the results of DIBK simulations for the energy loss of electrons and positrons under the same conditions as in the experiment. Figure 4 also shows the simulated energy-loss spectrum of 120 GeV/c electrons with a beam divergence of 150 μrad and the other parameters unchanged. It is evident that the energy-loss and radiation spectra in Fig. 4 are very similar, demonstrating that radiation is nearly independent of beam charge and divergence. Such features are explained by a similar dynamics for $e^{\pm}$ and for particles with different incidence angles with the crystal and, together with the high-intensity and wide spectrum, render this type of radiation attractive for applications. For instance, the e.m. radiation accompanying MVROC can be used to convert $e^{\pm}$ beams to γ radiation without strict requirements on crystal orientation and beam divergence.

Another advantage of a scheme for radiation generation relying on VR/MVROC is its robustness vs crystalline imperfections as compared to that of channeling-based effects [31]. Such a possibility also envisages the use for higher-Z materials, which are better than Si for e.m. generation, though they cannot be produced with the same perfection as a Si crystal. This feature could be exploited, for instance, for a positron source using MVROC in a tungsten crystal [32].

Provided that pair production under MVROC conditions maintains the wide angular acceptance as for photoproduction, the radiation accompanying MVROC could be used to reduce the thickness of crystalline electromagnetic calorimeters in HEP, such as the one of the Compact Muon Solenoid (CMS) [33], due to lowering of the length of the electromagnetic shower. The same principle can be used to render orbital gamma telescopes, such as the Fermi Gamma-Ray Space Telescope [34], more sensitive to the direction of celestial photons.

Finally possible applications that would exploit both the features of radiation and high deflecting power under

MVROC consist of a crystal-assisted collimation device and beam dump [35] for future linear $e^{\pm}$ colliders, such as the ILC. The collimation system of ILC will be mainly made by spoiler-absorber pairs for the extraction of halo particles, which may result in wakefield perturbations because of beam-spoiler interactions. The insertion of a *short* Si crystal (some mm) instead of a *long* spoiler (some cm or more) would diminish the wakefield perturbations. A proposal in this sense has already put forward by Seryi [36]. Such a collimation scheme consists of replacing one or more of the spoilers with curved crystals oriented with the beam under VR. The particles deflection by VR would increase halo-cleaning efficiency per unit of length as compared to the case of an amorphous spoiler. VR is preferable to channeling for such collimation due to its higher efficiency, large angular acceptance, and similar radiation spectrum for $e^{\pm}$. Moreover, the increase in energy loss due to VR vs that for the amorphous case would improve the discrimination of halo particles, which will be later deflected by outstream bending magnets. The greater deflection and energy lost by $e^{\pm}$ under MVROC than that for an individual VR makes the radiation accompanying MVROC still more suitable for crystal-assisted collimation.

In summary, the possibility to exploit bent crystals under MVROC conditions to generate wide-spectrum and very intense electromagnetic radiation has been demonstrated experimentally and well reproduced in simulations. Such radiation naturally combines multiple synchrotronlike and CB-like planar radiation with string of strings radiation mechanism. The experimental electron energy losses have been recorded, up to the nominal beam energy. The comparison with individual VR highlights that the spectrum of energy losses accompanying MVROC is harder and 3 times more intense. Such features provide interesting prospects for applications.

We are grateful to Professor L. Lanceri who provided the tracking detectors and to V. Carassiti and M. Melchiorri for the design and fabrication of the crystal holder. We recognize financial support by the INFN-ICE-RAD experiment.

[1] P. Elleaume, Beam Line **32-1**, 14 (2002).
[2] D. J. Scott *et al.*, Phys. Rev. Lett. **107**, 174803 (2011).
[3] M. L. Ter-Mikaelian, *High-Energy Electromagnetic Processes in Condensed Media* (Wiley, New York, 1972).
[4] A. I. Akhiezer and N. F. Shulga, *High-Energy Electrodynamics in Matter* (Gordon and Breach, New York, 1996).
[5] V. N. Baier, V. M. Katkov, and V. M. Strakhovenko, *Electromagnetic Processes at High Energies in Oriented Single Crystals* (World Scientific, Singapore, 1998).
[6] V. G. Baryshevskii and V. V. Tikhomirov, Usp. Fiz. Nauk **159**, 529 (1989) [Sov. Phys. Usp. **32**, 1013 (1989)].
[7] E. N. Tsyganov, Technical Publication Report No. FERMILAB-TM-0682, 1976.
[8] A. M. Taratin and S. A. Vorobiev, Phys. Lett. A **119**, 425 (1987).
[9] J. Lindhard, Phys. Lett. **12**, 126 (1964); J. Lindhard, K. Dan. Vidensk. Selsk. Mat. Fys. Medd. **34**, 1 (1965).
[10] Yu. A. Chesnokov, V. I. Kotov, V. A. Maisheev, and I. A. Yazynin, JINST **3**, P02005 (2008).
[11] V. A. Maisheev, Nuovo Cimento Soc. Ital. Fis. C **34C**, 73 (2011).
[12] S. Bellucci and V. A. Maisheev, Phys. Rev. **86**, 042902 (2012).
[13] W. Scandale *et al.*, Phys. Rev. A **79**, 012903 (2009).
[14] D. Lietti *et al.*, Nucl. Instrum. Methods Phys. Res., Sect. B **283**, 84 (2012).
[15] V. V. Tikhomirov, Phys. Lett. B **655**, 217 (2007).
[16] W. Scandale *et al.*, Phys. Lett. B **682**, 274 (2009).
[17] W. Scandale *et al.*, Phys. Lett. B **693**, 545 (2010).
[18] W. Scandale *et al.*, Europhys. Lett. **93**, 56002 (2011).
[19] V. M. Strakhovenko, Phys. Rev. A **68**, 042901 (2003).
[20] V. Guidi, A. Mazzolari, and V. V. Tikhomirov, J. Appl. Phys. **107**, 114908 (2010).
[21] V. Guidi, L. Bandiera, and V. V. Tikhomirov, Phys. Rev. A **86**, 042903 (2012).
[22] L. Bandiera *et al.*, Nucl. Instrum. Methods Phys. Res., Sect. B **309**, 135 (2013).
[23] S. Hasan, Ph.D. thesis, University of Insubria, 2011, http://cdsweb.cern.ch/record/1353904/files/Thesis-2011-Hasan.pdf.
[24] A. Berra, Ph.D. thesis, University of Insubria, 2012.
[25] L. Celano, D. Creanza, M. de Palma, G. Maggi, L. Fiore, V. Paticchio, G. Raso, G. Selvaggi, L. Silvestris, and P. Tempesta, Nucl. Instrum. Methods Phys. Res., Sect. A **381**, 49 (1996).
[26] S. Baricordi, V. Guidi, A. Mazzolari, D. Vincenzi, and M. Ferroni, J. Phys. D **41**, 245501 (2008).
[27] S. Baricordi *et al.*, Appl. Phys. Lett. **91**, 061908 (2007).
[28] V. Guidi, L. Lanzoni, and A. Mazzolari, J. Appl. Phys. **107**, 113534 (2010).
[29] W. Scandale *et al.*, Phys. Lett. B **681**, 233 (2009).
[30] V. Guidi, A. Mazzolari, and V. V. Tikhomirov, Nuovo Cimento Soc. Ital. Fis. C **34**, 63 (2011).
[31] E. Bagli *et al.*, Phys. Rev. Lett. **110**, 175502 (2013).
[32] X. Artru, V. N. Baier, R. Chehab, and A. Jejcicm, Nucl. Instrum. Methods Phys. Res., Sect. A **344**, 443 (1994).
[33] CMS Collaboration *et al.*, JINST **3**, S08004 (2008).
[34] W. B. Atwood *et al.*, Astrophys. J. **697**, 1071 (2009).
[35] R. Appleby, L. Keller, T. Markiewicz, A. Seryi, R. Sugahara, and D. Walz, *Proceedings of the 2005 International Linear Collider Physics and Detector Workshop and Second ILC Accelerator Workshop, Snowmass, Colorado, 2005*, econf C0508141, ILCAW0514 (2005).
[36] A. Seryi, Nucl. Instrum. Methods Phys. Res., Sect. A **623**, 23 (2010).
[37] V. V. Tikhomirov, Nucl. Instrum. Methods Phys. Res., Sect. B **36**, 282 (1989).